SURFACE DEFORMATION MONITORING USING TERRASAR-X INTERFEROMETRY

Sang-Wan Kim[1)], Shimon Wdowinski[2)], Tim Dixon[2)]

[1)] Dept. of Geoinformation Engineering, Sejong University,
98 Gunja-Dong Gwangjin-Gu, Seoul 143-747, Korea
[2)] Division of Marine Geology and Geophysics, University of Miami, Miami, Florida, USA
E-mail: swkim@sejong.ac.kr

ABSTRACT: TerraSAR-X is new radar satellite operated at X-band, multi polarization, and multi beam mode. Compared with C-band or L-band SAR, the X-band system inherently suffers from more temporal decorrelation, but is more sensitive to surface deformation monitoring due to short wavelength (3.1 cm) and high spatial resolution (1m-3m). It is generally expected that sensitivity to estimate surface movement using TerraSAR-X will be increased by the factor of 10, compared to current C-band system with low spatial resolution such as ERS-2, Envisat. Many urban areas are experiencing land subsidence due to water, oil and natural gas withdrawal, underground excavation, sediment compaction, and so on. Monitoring of surface deformation is valuable for effectively limiting damage areas. In addition high accuracy and spatially dense subsidence map can be achieved by X-band InSAR observation, promoting identification and separation of various subsidence processes and leading to enhanced understanding via mechanical modeling. In this study we will introduce some initial InSAR results using new TerraSAR-X SAR data for surface deformation monitoring.

KEY WORDS: Deformation, InSAR, SAR, X-band, TerraSAR-X

1. INTRODUCTION

Many urban areas are experiencing land subsidence due to anthropogenic activities, such as water, oil and natural gas withdrawal, and underground excavation (Amelung et al., 1999, Galloway et al., 1999; Hu et al., 2004; Dixon et al., 2006). In addition, some areas also experience subsidence due to natural processes such as sediment compaction (Kim et al., 2005). The impacts of land subsidence can be considerable and extensive damage to human society. Observation and prediction is valuable for effectively limiting damages from land subsidence.

High accuracy and spatially dense subsidence data, such as InSAR, can not only identify and separate various subsidence processes, but lead to enhanced understanding via mechanical modeling. Recently TerraSAR-X(TSX) was successfully launched, which provides new opportunity to investigate more detailed phenomenon of ground displacement in urban area by means of high spatial observation.

We modified and developed our codes based on Roi_Pac in order to apply InSAR technique to TSX SSC (Single Look Slant Range Complex) data. TerraSAR-X data over salt flat in Bolivia and New Orleans were used to test our new developed algorithm. Although we present here very initial X-band InSAR result only, due to the limitation of data availability, this study would provide useful test for the general feasibility and accuracy assessment of X-band SAR interferometry technique in urban and dried desert.

2. TERRASAR-X DATA AND PROCESSING

The six TerraSAR-X SSC data were selected for interferometric processing. All data were acquired from a stripmap mode with HH polarization. The two SSC data over salt flat in southwest Bolivia, distributed by DLR as an sample InSAR pair, were acquired on 2007-07-15 and 2007-07-26 at the incidence angle of 39° (strip_11), and the four SSC data over New Orleans were acquired at two different incidence angles of 26° (strip_005) and 28.5° (strip_006) between 2008-02-11 and 2008-04-06 (see Table 1 and Fig. 1). The Roi_Pac were utilized for whole interferometric processing of TerraSAR-X data followed by extracting the TSX's sensor parameters by Gamma ISP module. Although the Roi_Pac was originally developed and distributed by JPL (Rosen et al., ?), we modified many steps in order to improve the performance, to make it more robust in very flat area and mountainous area, and to deal with the data with inaccurate orbit such JERS-1 and RADARSAT-1. Fig. 2 shows the flowchart of the modified Roi_Pac, which was used for all steps of radar interferometry using TerraSAR-X data. The most special consideration on the processing of our data set is of offset estimation between master image and simulated SAR image derived from DEM. In a gently undulating area such as salt flat and New Orleans, co-registration often failed due to the lack of image contrast of simulated SAR image. Amplitude value of simulated SAR only represents the geometric effect of backscattering factor, which is calculated from input DEM. A reference image such as pre-geocoded SAR image or orthophoto image can be used as pseudo-simulated image. Here we used Landsat ETM panchromatic ortho-rectified image (Tucker et al., 2004). The 3-arc SRTM (Shuttle Radar Topographic Mission) DEM (Digital Elevation Data)

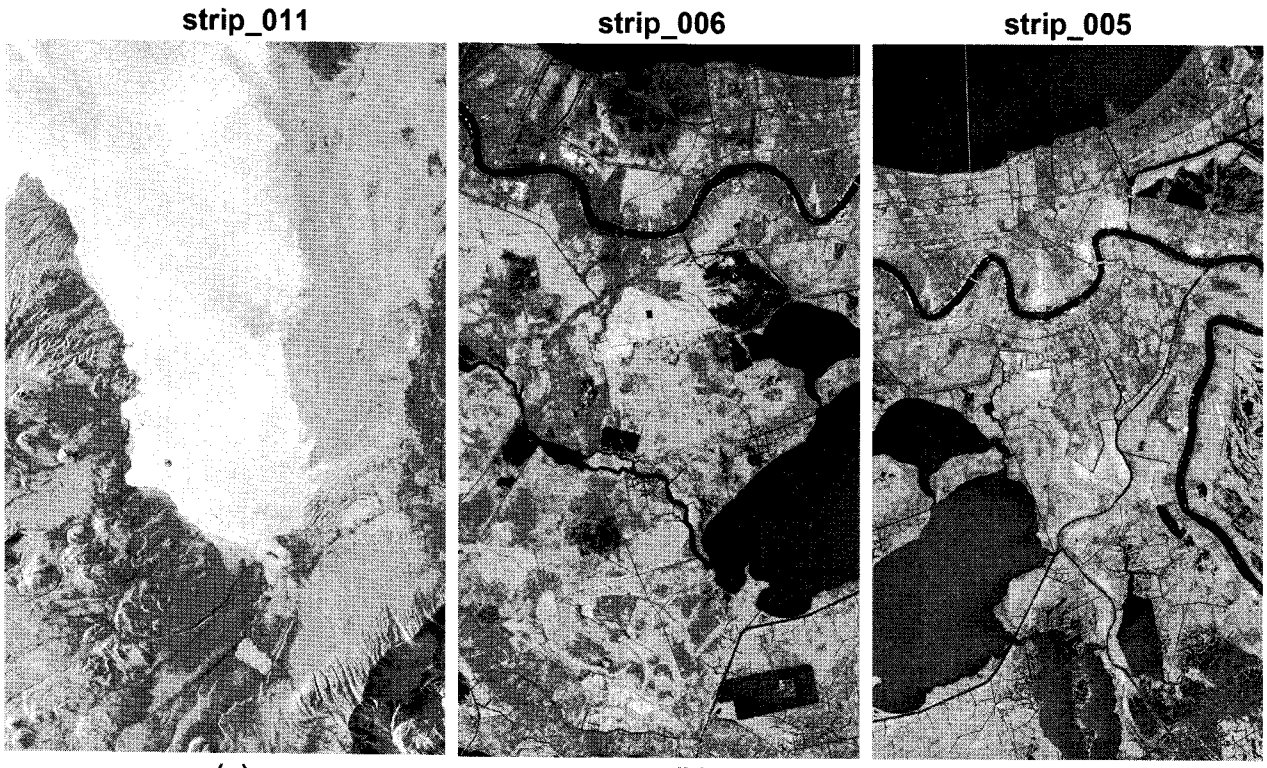

Fig. 1. (a) TerraSAR-X image over salt flat in southwest Bolivia acquired at HH polarization, stripmap 11, and TerraSAR-X image over New Orleans acquird at HH polarization, stripmap 6 (b) and stripmap 5 (c).

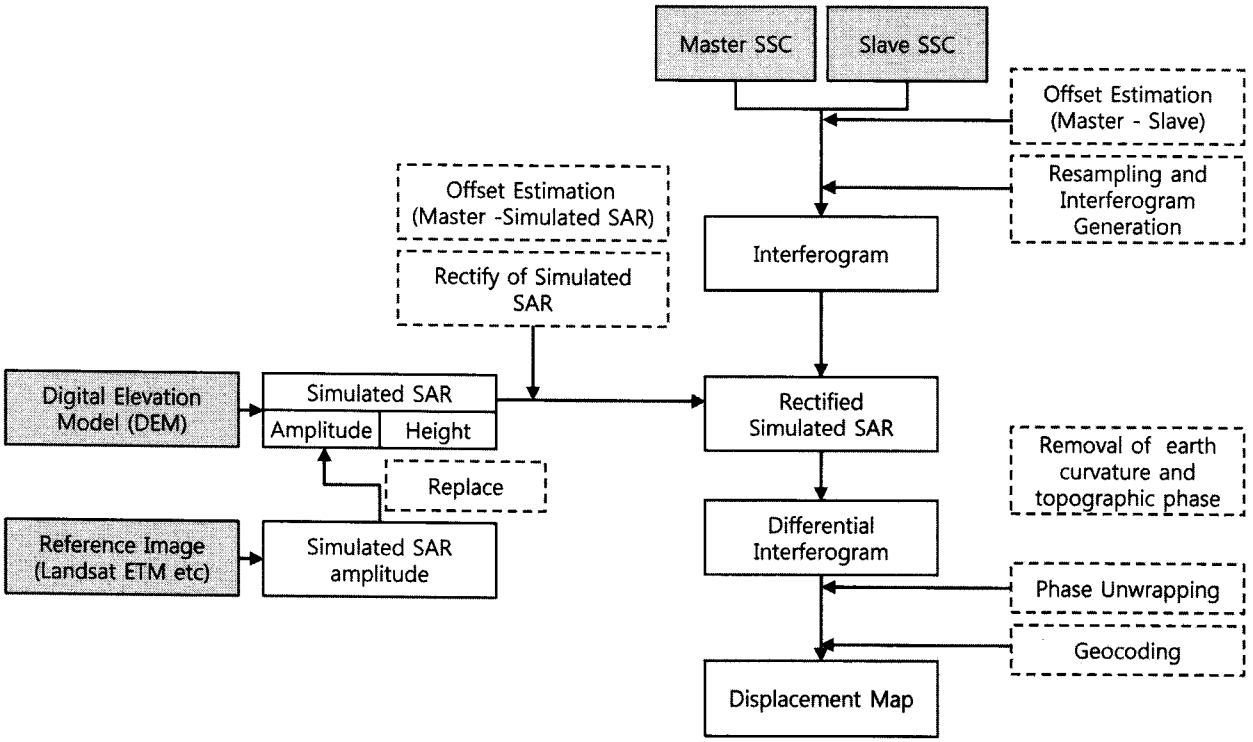

Fig. 2. Flowchart of differential SAR interferometric processing used in this study.

Table 1 List of TerraSAR-X data used for the study

Region	Date	Sensor Mode	Polari-zation	Relative Orbit	Beam
Salt flat in Bolivia	2007-07-15	Stripmap	HH	32	strip_011
	2007-07-26	Stripmap	HH	32	strip_011
Urban and wetland in New Orleans	2008-02-22	Stripmap	HH	158	strip_006
	2008-02-22	Stripmap	HH	158	strip_006
	2008-03-15	Stripmap	HH	158	strip_005
	2008-04-06	Stripmap	HH	158	strip_006

over salt flat in Bolivia and the 1-arc NED DEM over New Orleans in USA, provided from the USGS website (http://seamless.usgs.gov), was used to subtract topographic phase from interferogram.

3. RESULT AND DISCUSSION

Three differential interferograms were generated over the study area using TSX data. Figure 3 shows an amplitude image and radar-coordinated height image in salt flat that is derived from SRTM 3-arc DEM and pseudo-amplitude image derived from Landsat ETM panchromatic ortho-rectified image. The simulated SAR amplitude (Fig. 3a) was replaced with pseudo-amplitude image (Fig. 3c) for offset estimation with the master image (Fig. 1a). The differential interferometric phases without any orbit refinement are shown in Fig. 4, showing surface deformation and/or noise term including orbital fringe, DEM error, and atmospheric distortion. No significant residual fringe due to inaccurate orbit was observable since TSX provide very precise orbit. The temporal baselines of all interferometric pairs are 11-day and the perpendicular baselines is 858 m for 2007-7-15/2007-7-26 pair, 126 m for 2008-2-22/2008-4-6 pair, and 35 m for 2008-2-11/2008-3-15 pair.

As expected the high coherence is observable in the whole salt flat (Fig. 4a) and urban area (Fig. 4b and 4c) and surprisingly the medium coherence in wetland area (Fig. 4b and 4c). Many residual fringes with high spatial frequency in the southern part of Fig. 4a resulted from the used DEM error. The large perpendicular baseline of Bolivia pair leads the small altitude of ambiguity of about 20 m, which is sensitivity to topographic relief comparable to 2π in interferometric phase image. The fringe depending on DEM error can be used to improve the DEM accuracy. Meantime, the residual phase in salt flat (the upper part of Fig. 4a) may reflect surface deformation and/or atmospheric effect.

The southern part of 2008-2-11/2008-3-15 pair (Fig. 2(d)) and most area of 2008-2-22/2008-4-6 pair consist of wetland, showing a lot of dramatic change. It is likely that many of these fringes are associated with the water level change in wetland, considering the continuity and discontinuity of the pattern across an artificial structure. In general the fringe that is resulted from atmospheric effect does not interfered with a physical structure on surface while the fringe by water level change does.

Although our purpose of this study is to detect surface displacement using TerraSAR-X data with high spatial resolution, we could not apply any reasonable analysis at this time due to the limited number of interferogram. After acquiring more TSX data the stack of high resolution SAR data enable us to detect much more new information on surface displacement.

Acknowledgements

We thank DLR for access to the TerraSAR-X data.

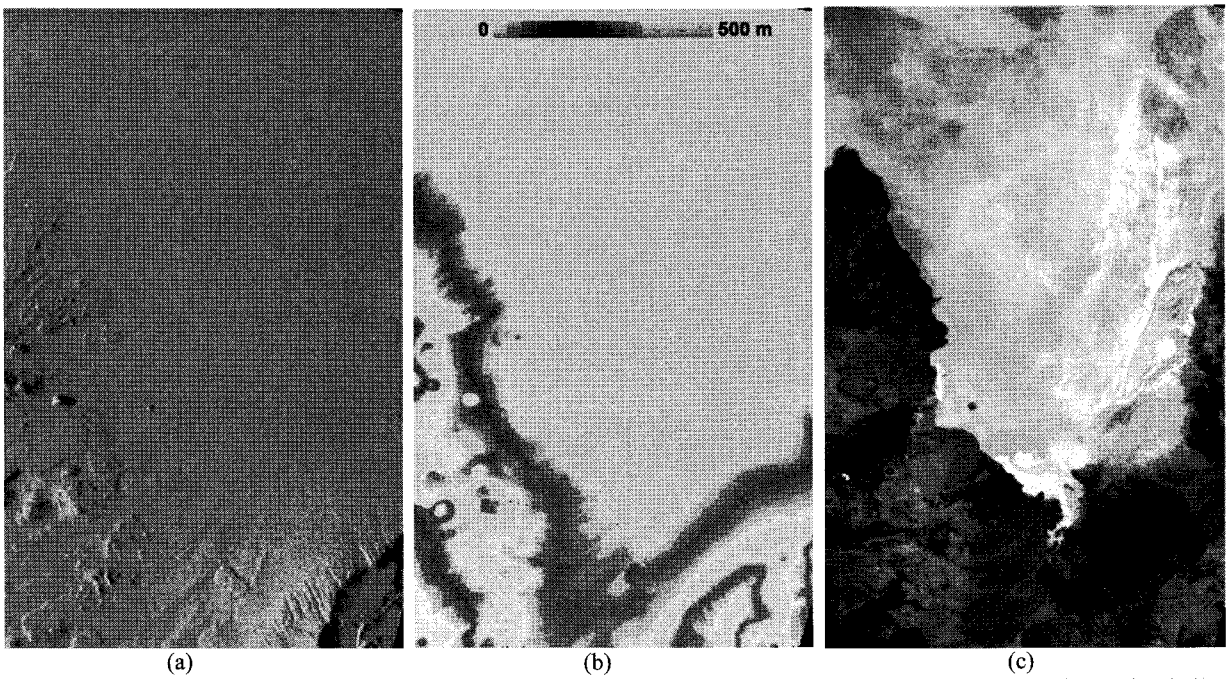

(a) (b) (c)

Fig. 3. (a) Amplitude image and (b) height image of simulated SAR derived from SRTM 3-arc DEM. (c) pesudo-amplitude image derived from Landsat ETM panchromatic ortho-rectified image.

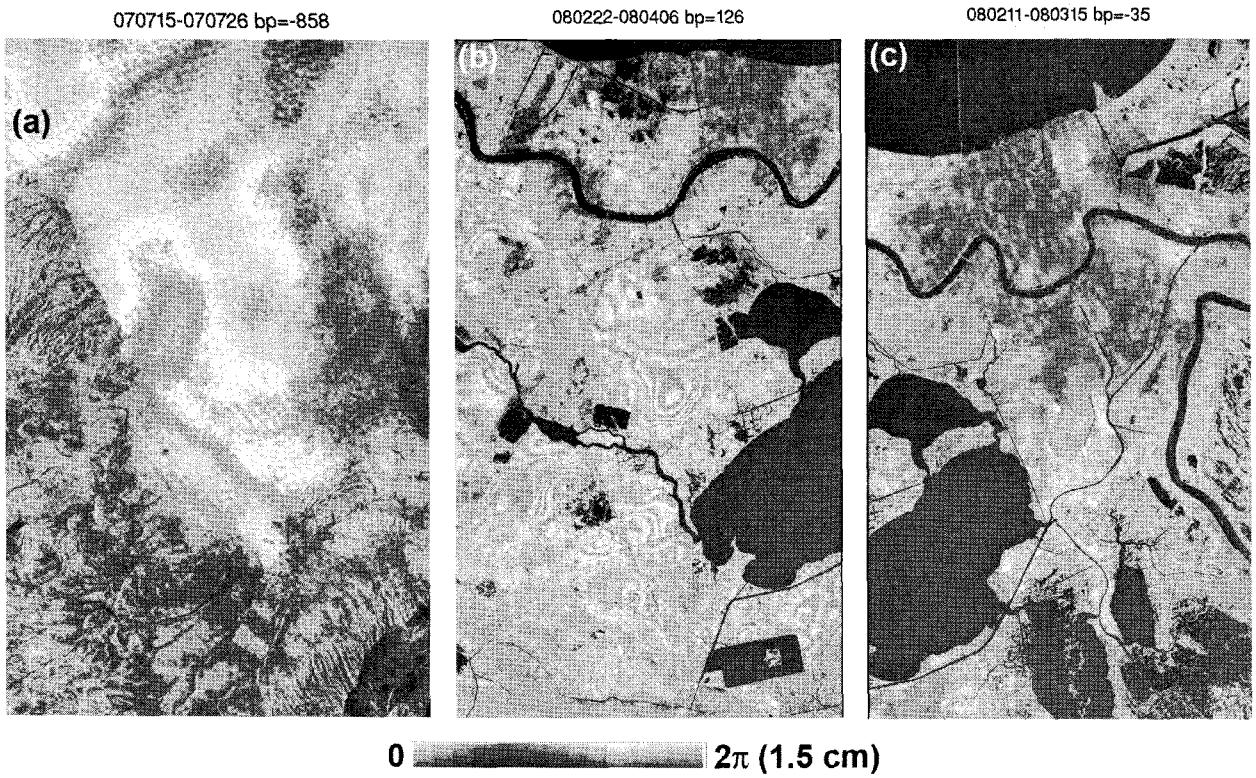

Fig. 4. Differential interferograms of TerraSAR-X interferometric pair: (a) 2007-7-15/2007-7-26 pair with the perpendicular baseline of -858 m. (b) 2008-2-22/20080406 pair with the perpendicular baseline of 126 m, (c) 2008-2-11/2008-3-15 pair with the perpendicular baseline of -35 m.

This work was supported by the KARI (Korea Aerospace Research Institute).

REFERENCES

Amelung, F., Galloway, D.L., Bell, J.W., Zebker, H.A., and Laczniak, R.J., 1999. Sensing the ups and downs of Las Vegas: InSAR reveals structural control of land subsidence and aquifer-system deformation. *Geology*, v. 27, pp. 483-486.

Dixon, T.H., Amelung, F., Ferretti, A., Novali, F., Rocca, F., Dokka, R., Sella, G., Kim, S.W., Wdowinski, S., and Whitman, D., 2006. Subsidence and flooding in New Orleans. *Nature*, 441, pp. 587-588.

Hu, R.L., Yue, Z.Q., Wang, L.C., and Wang, S. J., 2004. Review on current status and challenging issues of land subsidence in China. *Engineering Geology*, v. 76, pp. 65-77.

Galloway, D.L., Jones, D.R., & Ingebritsen, S.E., 1999. Land subsidence in the United States. In. Denver: USGS

Kim, S.W., Lee, C.W., Song, K.Y., Min, K.D., and Won, J.S., 2005. Application of L-band differential SAR interferometry to subsidence rate estimation in reclaimed coastal land. *International Journal of Remote Sensing*, v. 26, pp. 1363-1381.

Rosen, P.A., Hensley, S., Peltzer, G., and Simons, M., 2004. Updated Repeat Orbit Interferometry Package released. *EOS Transactions, AGU*, v. 85, pp. 47, 2004.

Tucker C.J., Grant D.M., and Dykstra J.D., 2004. NASA's global orthorectified landsat data set. *Photogrammetric Engineering and Remote Sensing*, v. 70, pp. 313-322.